CrossMark

The First Detection of X-Ray Polarization in a Newly Discovered Galactic Transient Swift J151857.0-572147

Santanu Mondal[1] , S. Pujitha Suribhatla[1], Kaushik Chatterjee[2] , Chandra B. Singh[2] , and Rwitika Chatterjee[3]
[1] Indian Institute of Astrophysics, II Block, Koramangala, Bengaluru 560034, Karnataka, India; santanuicsp@gmail.com
[2] South-Western Institue For Astronomy Research, Yunnan University, University Town, Chenggong, Kunming 650500, People's Republic of China
[3] Space Astronomy Group, ISITE Campus, U. R. Rao Satellite Center, ISRO, Bengaluru, 560037, India

Abstract

We study the spectropolarimetric properties of a newly discovered black hole (BH) X-ray binary Swift J151857. 0-572147 jointly using Imaging X-ray Polarimetry Explorer (IXPE) and NuSTAR observations during 2024 March. The analysis of IXPE data reports the first detection of X-ray with a polarization degree (PD) of 1.34 ± 0.27 and a polarization angle (PA) of $-13°69 \pm 5°85$ using a model-independent approach, while the model-dependent analysis gives a PD of 1.18 ± 0.23 and a PA of $-14°01 \pm 5°80$. The joint spectral analysis of the broadband data and NuSTAR analysis in isolation constrain the mass of the central BH between $\sim 9.2 \pm 1.6$ and $10.1 \pm 1.7 M_\odot$ and a moderate spin parameter of $\sim 0.6 \pm 0.1$–0.7 ± 0.2 with a disk inclination of $\sim 35° \pm 7°$–$46° \pm 15°$. The power-law photon index and cutoff energy are 2.19 ± 0.03–2.47 ± 0.06 and $\sim 36 \pm 4$–78 ± 10 keV, suggesting a transition to the soft spectral state. Additionally, a relatively lower corona size of 6 ± 1–$9 \pm 2 r_S$, a low mass outflow rate ($<3\% \dot{M}_{Edd}$), and the best-fitted halo accretion is less compared to the disk accretion rate further confirm the same state. The low PD detected in the soft state can be due to repeated scattering inside the dense corona, and the dominant emission from the disk agrees with the low spin and low disk inclination. The hydrogen column density obtained from the fit is relatively high at ~ 4–5×10^{22} cm^{-2}.

1. Introduction

Matter accreting onto a black hole (BH) forms an accretion disk consisting mainly of two components: the inner puffed-up region, which is known as the so-called corona, and the cold Keplerian disk. The first component upscatters soft photons from the Keplerian disk through inverse Comptonization, making them hard (R. A. Sunyaev & L. G. Titarchuk 1980; F. Haardt & L. Maraschi 1993; S. Chakrabarti & L. G. Titarchuk 1995; C. Done et al. 2007; S. Mondal & S. K. Chakrabarti 2013, and references therein). The same region also launches jet/outflows (S. K. Chakrabarti 1999; I. Chattopadhyay & S. Das 2007; S. Mondal & S. K. Chakrabarti 2021) and polarizes the radiation depending on its temperature, optical depth, geometry, and inclination (P. A. Connors et al. 1980; R. A. Sunyaev & L. G. Titarchuk 1985, and references therein). In addition to the above geometrical configuration and accretion properties, the spin of the BH is a crucial parameter in deciding the amount of polarization as well as its energy dependence. Therefore, the polarization properties, such as polarization angle (PA) and degree (PD) of any source, depend on several factors, including accretion properties and the spin of the BH. The variation of PD and PA on the optical depth, disk inclination, spin of the BH, and outflows was studied in detail both in theory and simulation (M. C. Begelman & C. F. McKee 1983; M. Dovčiak et al. 2008; L.-X. Li et al. 2009; J. D. Schnittman & J. H. Krolik 2010; H. Krawczynski 2012; R. Taverna et al. 2020; A. Ratheesh et al. 2024, and

references therein). Therefore, by constraining the coronal properties of a system, the PD can be constrained or vice versa along with the intrinsic parameters of the BH, making spectropolarimetric studies important in recent times.

Black hole X-ray binaries (BHXRBs) show variabilities in their spectral states during the outburst time (R. A. Remillard & J. E. McClintock 2006). In general, they follow a cycle starting from a hard state (HS) when spectra are dominated by hard photons from the corona region to a soft state (SS) when spectra are dominated by soft photons mainly from the disk through intermediate states (J. Homan et al. 2001; T. Belloni et al. 2005; R. A. Remillard & J. E. McClintock 2006; A. Nandi et al. 2012; D. Debnath et al. 2015; A. Jana et al. 2016; Q. C. Shui et al. 2021, and references therein). Sometimes, some of the sources may not follow the cycle for several reasons, e.g., lack of supply of matter or lack of viscosity, etc. (A. R. King 1998; S. Mondal et al. 2017; S. K. Chakrabarti et al. 2019; S. Mondal 2020). Outbursts that do not go to the SS (B. E. Tetarenko et al. 2016, and references therein) or do not pass through all states are called failed outbursts. In the SS, the disk moves much closer to the BH and the emission from the corona region is negligibly small. As the corona nearly disappears in the SS and its optical depth increases, it can trap more radiation, lowering the probability of hard emission (see R. A. Sunyaev & L. G. Titarchuk 1980; S. K. Chakrabarti 1997; S. Mondal & S. K. Chakrabarti 2013, and references therein). Therefore, the scattering can also affect the amount of polarization (R. A. Sunyaev & L. G. Titarchuk 1985).

The new Galactic transient Swift J151857.0-572147 (hereafter Swift J151857) was first detected by the Swift/X-Ray Telescope (XRT) as a gamma-ray burst (GRB 20240303A; J. A. Kennea et al. 2024a) in Swift Trigger 1218452[4] (GCN

___
[4] https://gcn.nasa.gov/circulars/35849

35849). However, its constant bright nature without signs of fading, along with its localization in the Galactic plane, was later confirmed to be a Galactic transient. From the best localization of the source using XRT immediate onboard localization, the R.A. and decl. of the source were found to be R.A. (J2000) = $15^h18^m57^s.00$ and decl. (J2000) = $-57^d21'47''.9$ (J. A. Kennea et al. 2024b). Follow-up radio observations with the MeerKAT telescope were done (F. J. Cowie et al. 2024) at 1.28 GHz (L band) with a bandwidth of 856 MHz at a flux density of 10 mJy (F. Carotenuto & T. D. Russell 2024) on 2024 March 4 for 15 minutes. The inverted radio spectrum ($f(\nu) \propto \nu^{\alpha}$, where $\nu \sim +0.5$) with the photon index helped designate the nature of the source as consistent with that of an X-ray binary in the HS, suggesting it may be a neutron star or a BH. The Australia Telescope Compact Array (ATCA) followed up on the radio observations on 2024 March 9 for $\sim$30 minutes at frequencies of 5.5 and 9 GHz simultaneously (P. Saikia et al. 2024). Their analysis also affirmed that the source was a Galactic BH. After the ATCA, Swift/XRT performed a target of opportunity on this source with an exposure of 1000 s. It was found that the spectrum is well described by the combination of phenomenological disk blackbody (diskbb) and power-law model (powerlaw) models (M. Del Santo et al. 2024). These findings also solidified the nature of the source as a BH. There was an INTEGRAL serendipitous detection of the source from 2024 March 8 to 11 (V. Sguera 2024). As part of the monitoring program of GRBs in optical and near-infrared wavelengths, the 60 cm Robotic Eye Mount telescope monitored the source in both of these wavelengths (M. C. Baglio et al. 2024).

The broadband X-ray data of the source from Insight-HXMT (S.-N. Zhang et al. 2020) was analyzed by K. Chatterjee et al. (2024) in the intermediate spectral state. The authors detected the presence of type-C quasiperiodic oscillations (QPOs) during the outburst period, which disappeared in the SS while the Imaging X-ray Polarimetry Explorer (IXPE; M. C. Weisskopf et al. 2016) observed the source. The Swift/XRT spectral modeling of the source reported a column density (N_H) of $5.6 \pm 0.06 \times 10^{22}$ cm^{-2} with a power-law photon index (Γ) of 1.78 ± 0.02 (see J. A. Kennea et al. 2024a). A similar N_H was estimated by K. Chatterjee et al. (2024). The negative velocity of an H I absorption line imposes the lower limit on the distance to the source to be $4.48^{+0.67}_{-0.47}$ kpc. While the absence of positive velocity absorption lines toward other sources in the field of the H I absorption for Swift J151857 puts an upper limit on the distance as $15.64^{+0.77}_{-0.60}$ kpc (B. J. Burridge et al. 2024). Due to a large uncertainty in distance estimation, we used an average distance of 10 kpc throughout our analysis for this source. Other information like the mass, inclination, and spin have not been reported about the source yet. From our analysis, we report these intrinsic properties of the source for the first time.

Recently, IXPE has observed several BHXRBs along with Swift J151857 and showcased their X-ray polarization detection. In 4U 1630-47, a PD of $\sim$6.5%–10% was observed (R. Cavero et al. 2023; A. Kushwaha et al. 2023a; D. Rawat et al. 2023; N. A. Ratheesh et al. 2024), in the HS of Swift J1727.8-1613 the PD measured $\sim$3%–4% (A. Ingram et al. 2023; A. Veledina et al. 2023; J. Podgorný et al. 2024), while a rapid decrease in PD of $\sim$0.5% was observed by J. Svoboda et al. (2024a) in the SS. In LMC X-3, $\sim$3% polarization was detected (J. Svoboda et al. 2024b; S. Majumder et al. 2024) and in the SS of 4U 1957 + 115 measured PD

was $\sim$1.95% (A. Kushwaha et al. 2023b; L. Marra et al. 2024). A 4% PD was detected in Cyg X-1 in the HS and 2.5%–2.8% in the SS (H. Krawczynski et al. 2022; A. Jana & H.-K. Chang 2024). Very recently, A. Veledina et al. (2024) detected a high polarization $\approx$25% in Cyg X-3 using IXPE observation. These studies not only detected polarization but also showed the variation in PD in different spectral states, as expected from the simulations. Therefore, there has been renewed interest in studying BHXRBs to further understand their accretion geometry, emission mechanisms, and intrinsic parameters of the central BH. The Swift J151857 source was observed by NuSTAR (F. A. Harrison et al. 2013) simultaneously with IXPE.

Motivated by recent X-ray polarization detections, which have been used as a powerful tool to understand several emission and accretion properties of BHXRBs, in this paper, we performed spectropolarimetric studies of Swift J151857. We used both IXPE and NuSTAR observations of the source to carry out broadband spectral and polarimetric studies to understand the origin of X-ray polarization, its properties, spectral states, accretion geometry, and intrinsic parameters of the BH. Along with the corona properties, we have also estimated the mass outflow from this system that connects the disk-corona outflow with polarization in a single framework. The paper is organized as follows: In Section 2, we discuss the observation and data reduction procedure. In Section 3, we discuss the spectropolarimetric data analysis results, and the origin of the detected polarization, and finally, we draw our conclusions in Section 4.

2. Observation and Data Reduction

The source Swift J151857 was observed on 2024 March 18 by IXPE with an exposure time of 96 ks and NuSTAR observed on March 17 and 18 (hereafter, epochs N1 and N2) with exposures of 14 and 9 ks, respectively. We present the analysis of the data from both days in this paper. The corresponding observation IDs are 03250201 (as epoch I), 91001311002 (as epoch N1), and 91001311004 (as epoch N2).

IXPE is an imaging X-ray telescope consisting of three polarization-sensitive detector units (DUs) that observe in the 2–8 keV energy range. We obtained the Level-2 event files from the HEASARC archive,[5] which are cleaned and calibrated using standard FTOOLS tasks with the latest calibration files (CALDB 20230526) available in the IXPE database. For extracting the source region, we select a circular region of 50″ for all detectors.

For NuSTAR analysis, we considered the observations from 2024 March 17 and 18 and have used the standard NUSTARDASv1.3.1[6] software to extract the data. We generated cleaned event files using the NUPIPELINE task and generated the spectra using NUPRODUCTS along with CALDB v20220331. We considered a region of 60″ for the source and 120″ for the background using DS9 (W. A. Joye & E. Mandel 2003). Furthermore, we used the grppha command to group the data with a minimum of 200 counts in each bin. We used the data of IXPE in the 2–8 keV range and NuSTAR data in the 3–79 keV energy range for each respective epoch of observation. For spectral analysis, we used XSPEC[7]
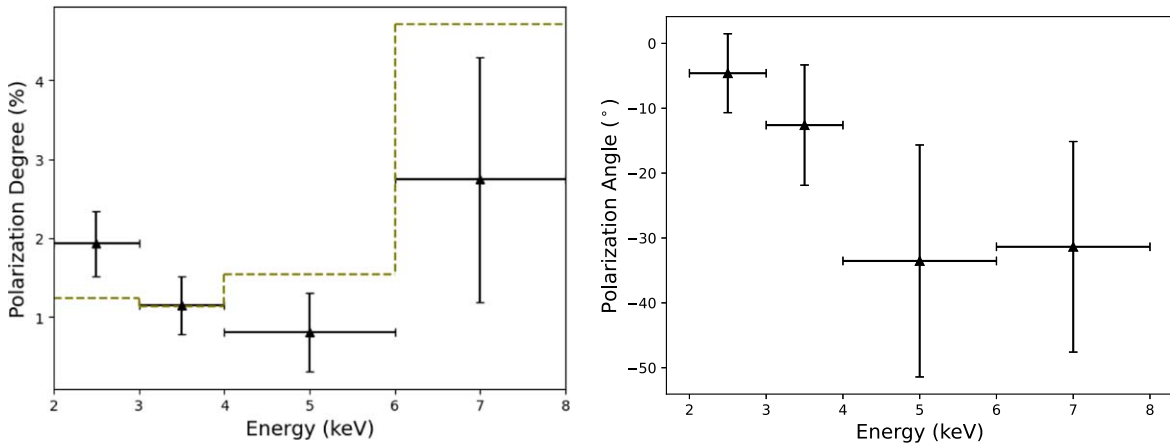
Figure 1. Energy-dependent PD and PA plots in the 2–8 keV energy range shown with 1σ error bars. The olive dashed line in the left panel represents the estimate of the MDP_{99}%.

Table 1
Results of Model-independent Polarimetric Analysis Performed Using the PCUBE Algorithm

Parameter	2–3 (keV)	3–4 (keV)	4–6 (keV)	6–8 (keV)	2–8 (keV)
Q/I (%)	1.90 ± 0.41	1.04 ± 0.37	0.31 ± 0.50	1.25 ± 1.55	1.19 ± 0.27
U/I (%)	-0.30 ± 0.41	-4.92 ± 0.37	-0.75 ± 0.50	-2.43 ± 1.55	-0.61 ± 0.27
PD (%)	1.93 ± 0.41	1.15 ± 0.37	0.81 ± 0.50	2.74 ± 1.55	1.34 ± 0.27
PA (°)	-4.60 ± 6.08	-12.60 ± 9.28	-33.54 ± 17.88	-31.36 ± 16.23	-13.69 ± 5.85
MDP_{99} (%)	1.24	1.13	1.54	4.71	0.83

(K. A. Arnaud 1996) v12.12.0. The χ^2 statistic is used for the goodness of the fit throughout the analysis. The best-fitted spectral plots are further rebinned for visual clarity; they neither affect the model parameter values nor the goodness of the fit.

3. Results and Discussions

3.1. Model-independent IXPE Analysis

The IXPEOBSSIM software v30.6.3[8] (L. Baldini et al. 2022) is used for the polarimetric analysis of the Level-2 IXPE data obtained from the HEASARC archive. The XPSELECT task is used to extract the source event lists. We did not carry out background subtraction for this source since it is very bright with an average flux of $\sim 1.40 \pm 0.02 \times 10^{-8}\,\mathrm{erg\,cm^{-2}\,s^{-1}}$. The model-independent PCUBE algorithm of the XPBIN task (F. Kislat et al. 2015) is used to obtain the polarization cube parameters in the 28 keV energy range. We also used the PHA1, PHA1Q, and PHA1U algorithms of the XPBIN task to obtain the Stokes I, Q, and U spectra of the source. To study any possible energy dependence of these parameters, we grouped the 2–8 keV data into four energy bands of 2–3, 3–4, 4–6, and 6–8 keV energy ranges and extracted the polarization parameters. We used a similar approach as discussed in R. Chatterjee et al. (2023) and S. Mondal et al. (2024).

The results of the model-independent polarimetric analysis are summarized in Table 1. The measured PD and PA in 2–8 keV are 1.34 ± 0.27 and $-13°.69 \pm 5°.85$, respectively. We have also performed energy-dependent PD and PA analyses,

which are shown in the left and right panels of Figure 1, respectively. As can be observed, the polarization measurements decrease with increasing energy and drop below the MDP_{99}% above 4 keV. This also gives the PD upper limit (99% confidence level, shown by the olive dashed line) of <1.54% and <4.71% in the 4–6 and 6–8 keV bands. The 1σ confidence contours between PA and PD for different energy bands are shown in Figure 2, obtained using the PCUBE algorithm. The errors obtained through the PCUBE algorithm do not include systematic (F. Kislat et al. 2015).

Our detected low PD for the source Swift J151857 in the SS is in agreement with the measurements of PD from other BHXRBs in the same state, e.g., $\sim$0.5% in Swift J1727.8-1613 (J. Svoboda et al. 2024a) and $\sim$1.95% in 4U 1957 + 115 (L. Marra et al. 2024). Additionally, an energy-dependent PD variation shows a decreasing trend, where the first two energy bands are above or within the minimum detectable polarization (MDP), while the higher energy band measurements are below the MDP. Such a decreasing profile in PD has been obtained from theory as well as from numerical simulations and that can be due to the following reasons. The spectra from accretion disks around BHs consist of mainly two types of photons: the low-energy photons that are emitted from the outer region of the disk, where the temperature is lower, and the effect of gravity is less important, whereas high-energy emissions are coming from the inner hot region of the disk, where the photon polarization is mostly affected by general relativistic effects. It was shown from numerical simulations that for higher optical depths (see, e.g., M. Dovčiak et al. 2008; H. Krawczynski 2012; R. Taverna et al. 2020; L. Marra et al. 2024), which is the case in the SS, direct radiation turns out to be polarized perpendicularly to the disk symmetry axis at lower energies,

---

[8] However, we note that a different version of the software gives different results, specifically, a nondetection of polarization using v30.6.4. Therefore, these results are solely based on the abovementioned version.
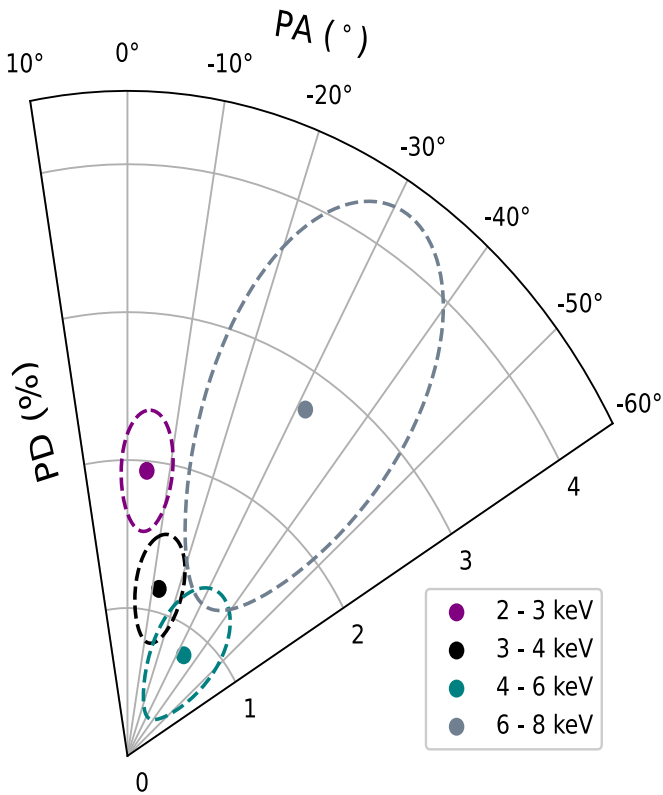
Figure 2. Contour plots between PD and PA obtained using the `PCUBE` algorithm in the 2–3, 3–4, 4–6, and 6–8 keV energy ranges. All contours are drawn with 1□ confidence.
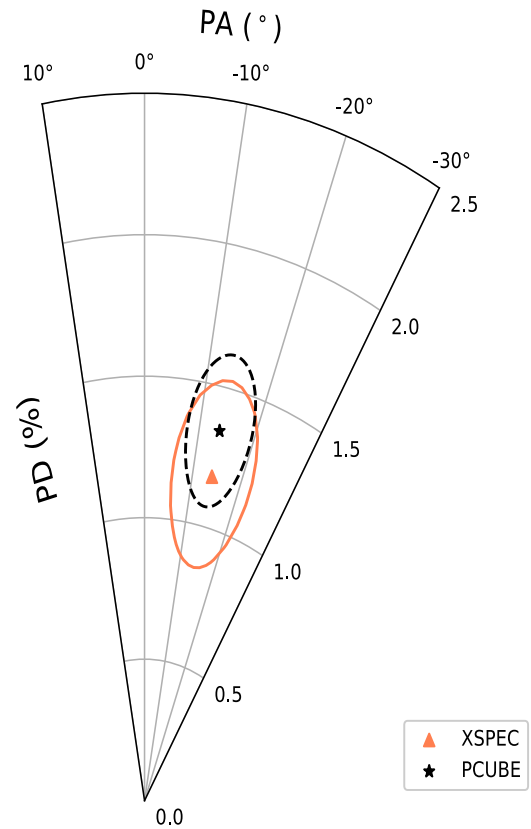

Figure 3. Contour plot between PD and PA with 1σ confidence, obtained using the `PCUBE` algorithm (model-independent) and XSPEC (model-dependent) fitting method.

while it slowly decreases at higher energies (>2 keV) under the effect of the polarization plane rotation. Such turnover energy is decided depending on the spin of the BH and the disk inclination. For higher spinning or inclination systems, turnover occurs at much closer energy and both PA and PD start increasing. However, our source has low inclination and spin (see Section 3.4); therefore, the decreasing PA and PD profiles and turnover around 5 keV are well in agreement with the theory and simulation.

Most of the IXPE observations for other BHXRBs showed nearly a constant PA. However, we found a decrease in PA with energy, which is similar to what was observed in 4U 1957 + 115 (A. Kushwaha et al. 2023b; L. Marra et al. 2024). Such a change in PA could be an indication of rotation of PA between 2 and 8 keV due to the effects of depolarization. Another possibility can be due to the orientation of jets. However, at present, the jet position angle is not well constrained for this source to compare with the detected PA, requiring a further jet study.

3.2. Model-dependent IXPE Analysis

For the model-dependent polarization study, we have fitted all Stokes spectra for epoch I using the absorbed `powerlaw`+`diskbb` model convolved with a constant polarization `polconst`, which reads in XSPEC as const*tbabs*pol-const*(powerlaw+diskbb). All Stokes spectra for all three DUs in the energy band of 2–8 keV are fitted simultaneously. The above model gives an acceptable fit with $\chi^2/\text{dof} = 1706/1332$. We determine the PA $= -14°.01 \pm 5°.80$ and the PD (%) $= 1.18 \pm 0.23$. Both of these values are in excellent agreement with the values obtained from the `PCUBE`

algorithm. The neutral hydrogen column density N_H is $5.58 \pm 0.13 \times 10^{22}$ cm^{-2}, obtained from the `tbabs` model. The `powerlaw` model photon index (Γ) and disk temperature in the `diskbb` model are 3.68 ± 0.08 and 0.97 ± 0.02 keV, respectively. High values of these two parameters may indicate that the source possibly moved to the soft spectral state during this observation epoch. The source was very recently studied in a follow-up work by K. Chatterjee et al. (2024) using Insight-HXMT data and observed the disappearance of QPOs in the SS during the epochs that coincide with IXPE observations, thereby further confirming our finding. The confidence contours from the model-dependent analysis are shown in Figure 3. The solid and dashed contours drawn using XSPEC and PCUBE, respectively, correspond to 1σ confidence.

Moreover, as the source moved to the SS, the inner disk moved much closer to the BH, and the corona became highly shrunk, 6–9 r_S ($2GM_\text{BH}/c^2$) (see Section 3.5) in comparison to HS in other BHXRBs (a few 100 r_S) (see S. Mondal et al. 2014; D. Debnath et al. 2015, and references therein). In the SS, it is widely believed that the accretion disk extends down to the innermost stable circular orbit (C. S. Reynolds 2019, for a review) and the spectrum is dominated by photons emitted from the very inner region, where the strong gravity can significantly alter the observed polarization properties (H. Krawczynski 2012; R. Taverna et al. 2020, and references therein). In this regime, the general relativistic effects cause the photon polarization vectors to undergo rotation, resulting in a net depolarization of the emission at infinity and an overall rotation of the PA. These effects are expected to be stronger for the high-energy photons emitted closer to the central BH,
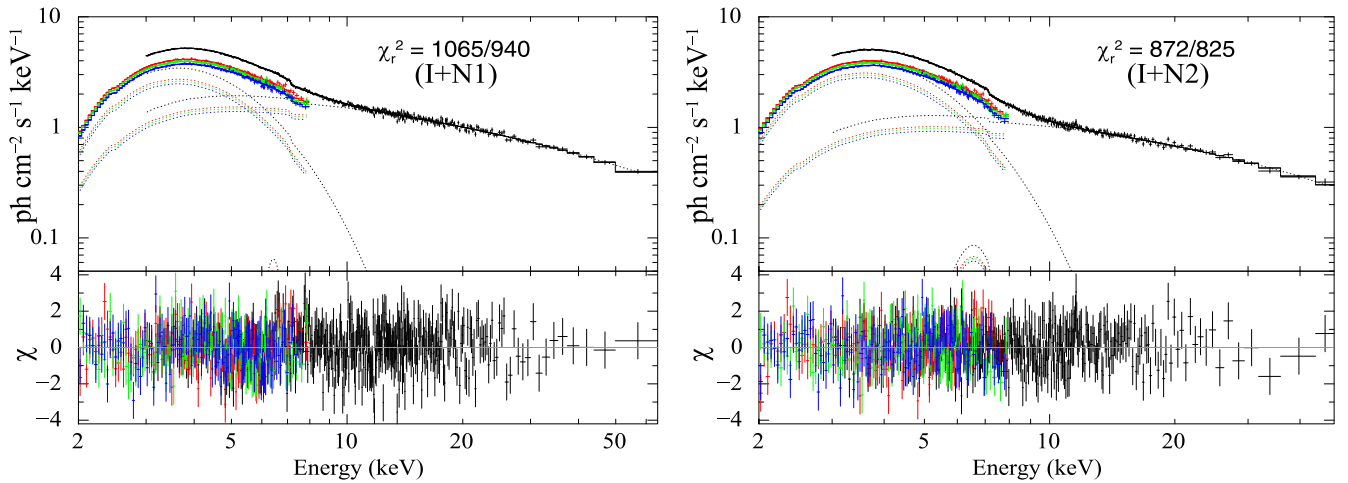
Figure 4. Joint spectral modeling of IXPE and NuSTAR data fitted using `cutoffpl+kerrbb` model in the energy band of 2–79 keV. The left and right panels are for the epochs (I+N1) and (I+N2). The Fe Kα line ∼6.4 is fitted using `the gauss` model. The blue, red, and green points correspond to IXPE data for all three DUs and the black points correspond to NuSTAR data. Plots are rebinned for visual clarity. See the text for details.

introducing the observed energy dependence of PD for this source in the SS. Numerical simulation performed in the literature (J. D. Schnittman & J. H. Krolik 2010; H. Krawczynski 2012; R. Taverna et al. 2020; L. Marra et al. 2024), showed a similar decreasing profile of PD and PA with energy and that also explains the case of low-spinning BH, which is valid for our source. Therefore, we do expect such a profile in PD for our source, if possible, to other sources in the future during the IXPE era. However, for a rapidly spinning BH with high inclination, an opposite PD profile is expected that agrees with the observed PD profile in, e.g., 4U 1957 + 115 in the SS.

We note that polarization measurement changes with spectral states, as we mentioned earlier. Two sources showed a significant change in PD in different spectral states: one is Cyg X-1 (H. Krawczynski et al. 2022; A. Jana & H.-K. Chang 2024) and the other Swift J1727.8-1613 (J. Svoboda et al. 2024a). These sources also showed significant detection of polarization in the SS, however, PD in the SS was much less compared to the HS. The number of scattering in the SS increases as photons get trapped by the scattering medium; thereby, polarization may decrease. J. Podgorny et al. (2023) detected ∼1.1% polarization in the SS of LMC X-1 and preferred a slab geometry of the corona. Our detection of PD in the SS is in accord with the above findings and further supports that the changes in spectral states are possibly followed by the changes in polarization properties. The possible origin of such low polarization favors the scenario in which the X-ray polarization is driven by the geometry of the accretion flow in the innermost region and an optically thick corona. Also, the polarization of the disk is perpendicular to that of the corona. As the disk emission dominates in the SS, the PD could decrease, as was explained in H. Krawczynski et al. (2022).

3.3. Joint IXPE and NuSTAR Analysis

For the broadband spectral analysis of the source, we performed a joint fitting using the simultaneous observations from IXPE in the 2–8 keV range and NuSTAR in the 3–79 keV energy range. We used a `const` component for a cross-calibration factor between NuSTAR and IXPE. The broadband energy range (2–79 keV) covered by the spectra of Swift J151857 showed a relatively broad Fe Kα line for which a Gaussian component (`gauss` model) is used at ∼6.4 keV.

We included a `tbabs` (J. Wilms et al. 2000) component to account for interstellar absorption. The data analysis is also performed using NuSTAR data in isolation as well. We carried out spectral analysis using both relativistic and nonrelativistic accretion disk models independently to estimate the accretion parameters as well as the intrinsic parameters of the central BH.

3.4. Kerrbb Model

A `kerrbb` (L. Li et al. 2005) component is used to characterize the emission from an accretion disk, including relativistic effects. This component models the radiation from a geometrically thin and optically thick accretion disk, as proposed by I. D. Novikov & K. S. Thorne (1973). The `cutoffpl` component was included to account for the Comptonized emission, which originates from the inner hot region of the disk or the corona. The total model reads in XSPEC as `const*tbabs*(gauss+cutoffpl+kerrbb)`. To take into account the calibration issues, as noted for other BH systems (see, e.g., N. R. Cavero et al. 2023; J. Podgorny et al. 2023; L. Marra et al. 2024), we used the `gain fit` command in XSPEC to adjust the response file gains of both telescopes. The same procedures were applied for both epochs.

In Figure 4, we show the model-fitted spectra of Swift J151857 for the joint IXPE and NuSTAR observations. The left and right panels show the spectral fits for the epochs I +N1 and I+N2. The lower panels show the residuals. As we did not have the mass, spin parameters of the BH, and the disk inclination beforehand, we left them free during model fitting, keeping the distance to the source fixed at 10 kpc. However, parameter values may change if the source distance changes significantly. Both data fits returned consistent values of all three parameters in both epochs. The mass (M_{BH}) and spin (a) parameters estimated from the fit vary between ∼9.2 ± 1.6 and 10.1 ± 1.7$M_\odot$ and 0.60 ± 0.12–0.69 ± 0.17, respectively. It possibly indicates that the BH is moderately rotating. The disk inclination (i) and the mass accretion rate obtained from the fit vary between ∼35° ± 7° and 46° ± 15° and (3.0 ± 0.3–4.0 ± 0.5) × 10^{18} gm s^{-1}. The low cutoff energy (E_c) of 36 ± 4–78 ± 10 keV with a photon index (Γ) of ∼2.19 ± 0.03–2.47 ± 0.06 indicates a transition to the soft spectral state of the source during the observation epoch after ejecting a high radio flare in the first week of March. The best-fitted model
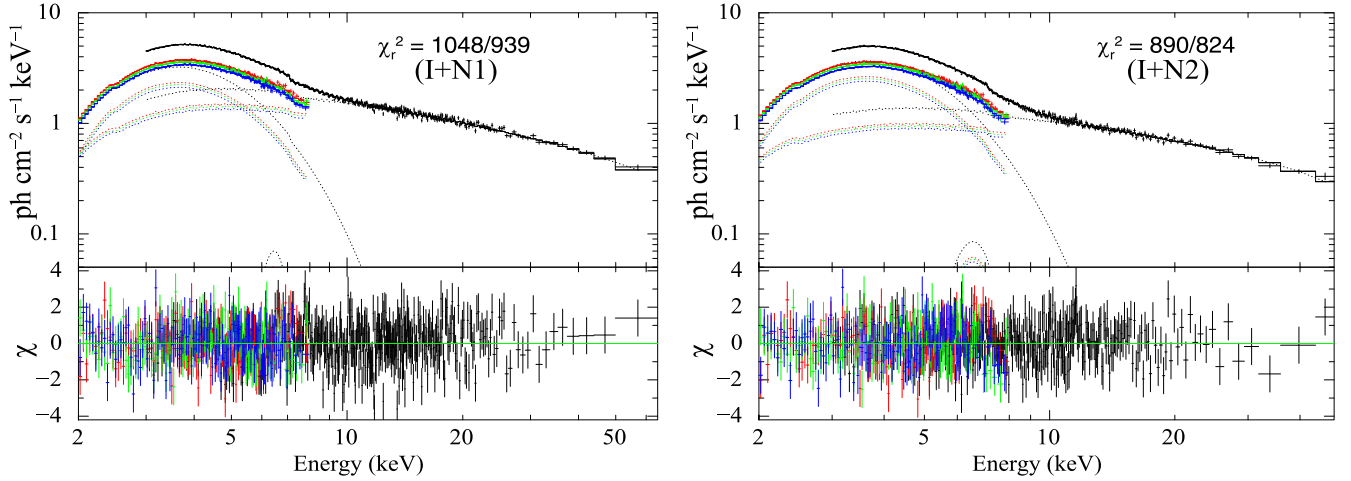
Figure 5. Joint spectral modeling of IXPE and NuSTAR data fitted using `diskbb+JeTCAF` model in the energy band of 2–79 keV. The left and right panels are for the epochs (I+N1) and (I+N2). The Fe Kα line ~6.4 is fitted using the `gauss` model. The blue, red, and green points correspond to IXPE data for all three DUs and the black points correspond to NuSTAR data. Plots are rebinned for visual clarity. See the text for details.

Table 2
Joint IXPE and NuSTAR, and Independent NuSTAR Spectra of Swift J151857 Fitted `cutoffpl+kerrbb` Model Parameters

Model →	kerrbb				cutoffpl		gauss	
Epoch ↓	a	i (°)	M_{BH} ($M_\odot$)	$\dot{m}_d$ (10^{18} gm s^{-1})	Γ	E_C (keV)	σ_g (keV)	χ^2/dof
I+N1	0.65 ± 0.17	35.2 ± 7.4	9.2 ± 1.6	3.76 ± 0.46	2.47 ± 0.06	78.4 ± 9.8	0.27 ± 0.12	1065/940
I+N2	0.62 ± 0.08	38.4 ± 6.3	9.7 ± 1.3	4.04 ± 0.47	2.37 ± 0.10	51.2 ± 8.9	0.67 ± 0.13	872/825
N1	0.69 ± 0.17	46.4 ± 15.0	10.1 ± 1.7	2.97 ± 0.31	2.30 ± 0.08	57.1 ± 6.7	0.28 ± 0.07	596/504
N2	0.60 ± 0.12	40.0 ± 9.3	9.3 ± 1.4	4.03 ± 0.19	2.19 ± 0.03	35.7 ± 4.3	0.41 ± 0.11	421/389

Note. We have fixed the following parameters: distance $D = 10$ kpc, spectral hardening factor $(hd) = 1.7$, Gaussian Fe K line energy = 6.4 keV. N_H obtained from both fits is ~ 4–5×10^{22} cm^{-2}.

parameters are given in Table 2. The N_H value of the source was high $\sim 3.6 \pm 0.5$–$5.3 \pm 0.4 \times 10^{22}$ cm^{-2}, which can be due to strong outflows from the outer disk or due to the presence of some blobs along the line of sight that can block the central radiation (see J. Neilsen & J. Homan 2012; S. Mondal & V. Jithesh 2023), requires further study of the outflows from the outer disk. We observed a broad Fe Kα width, which varies between 0.27 and 0.67 keV. It is expected as the source moved to the SS, the disk also moved closer to the BH; therefore, relativistic effects can broaden the line (see, e.g., A. C. Fabian et al. 1989; K. Iwasawa et al. 1996; L. W. Brenneman & C. S. Reynolds 2006; S. Mondal et al. 2016, and references therein). How close has the disk moved inward toward the BH? What is the corona geometry (radius and height)? This is studied in the next section.

The `kerrbb` model-fitted parameters infer that the source is possibly a moderately spinning BH with a low disk inclination. It has an impact on getting low PD measurements in IXPE data, as discussed in Sections 3.1 and 3.2. If we compare other sources that were observed with high PD in the SS, e.g., 4U 1630-47 ($i \sim 75°$) and LMC X-3 ($i \sim 69°$) are high inclination, on the contrary, Cyg X-1 and Swift J1727.8-1613 showed low PD having low inclination. Our source falls in the second type and the low PD can be attributed either to the repeated scattering of the trapped radiation in an optically thick medium or the polarization of the disk is perpendicular to the corona in

the SS (H. Krawczynski et al. 2022; J. Svoboda et al. 2024a, and references therein).

3.5. *JeTCAF* Model

To understand the accretion and outflow properties, we have further fitted the data using an accretion-ejection based two-component advective flow (S. Chakrabarti & L. G. Titarchuk 1995) model including a jet/outflows component (`JeTCAF`) (S. Mondal & S. K. Chakrabarti 2021). The `JeTCAF` model takes into account the radiation mechanisms at the base of the jet/outflows and the bulk motion effect by the outflowing jet on the emitted spectra, in addition to the Compton scattering of soft disk photons by the hot electron cloud inside the corona. The `JeTCAF` model has six parameters, namely, (i) the mass of the BH (M_{BH}) if it is unknown, (ii) the Keplerian disk accretion rate ($\dot{m}_d$), (iii) the sub-Keplerian halo accretion rate ($\dot{m}_h$), (iv) the size of the dynamic corona or the location of the shock (X_s in units of r_S), (v) the shock compression ratio (R), and (vi) the outflow collimation factor (f_{col}), the ratio of the solid angle subtended by the outflow to the inflow (Θ_o/Θ_{in}). The full model reads in XSPEC for IXPE and NuSTAR as `const*tbabs*(diskbb+gauss+JeTCAF)`.

Figure 5 shows the `JeTCAF` model-fitted spectra for both epochs. The $\dot{m}_d$ and $\dot{m}_h$ values obtained from the fit range between $\sim 0.72 \pm 0.03$ and 0.86 ± 0.03 and $\sim 0.23 \pm 0.02$–0.27 ± 0.02. The disk moved much closer to the BH with a corona radius of $\sim 6 \pm 1$–9 ± 2 r_S and f_{col}

Table 3
Joint IXPE and NuSTAR, and Independent NuSTAR Spectra Fitted `diskbb+JeTCAF` Model Parameters

| Model → | diskbb | JeTCAF | | | | | | gauss | |
Epoch ↓	T_{in} (keV)	M_{BH} ($M_\odot$)	$\dot{m}_d$ ($\dot{m}_{Edd}$)	$\dot{m}_h$ ($\dot{m}_{Edd}$)	X_s (r_S)	R	f_{col}	σ_g (keV)	χ^2/dof
I+N1	0.96 ± 0.01	9.8 ± 1.5	0.74 ± 0.04	0.25 ± 0.01	8.7 ± 1.5	6.67 ± 0.55	0.06 ± 0.02	0.41 ± 0.13	1048/939
I+N2	0.96 ± 0.02	9.6 ± 1.2	0.72 ± 0.03	0.23 ± 0.02	7.9 ± 1.1	4.97 ± 0.21	0.09 ± 0.01	0.63 ± 0.17	890/824
N1	0.97 ± 0.04	9.3 ± 1.3	0.86 ± 0.03	0.27 ± 0.02	6.6 ± 1.1	5.77 ± 0.43	0.06 ± 0.01	0.27 ± 0.09	583/503
N2	0.94 ± 0.03	9.2 ± 1.0	0.81 ± 0.04	0.23 ± 0.02	6.0 ± 1.1	5.48 ± 0.37	0.09 ± 0.01	0.54 ± 0.14	416/388

Note. All data sets required the gauss model for the Fe Kα line $\sim$6.4 keV of width σ_g given in the table. N_H obtained from both fits is $\sim$4–5 $\times 10^{22}$ cm^{-2}.

$\sim 0.06 \pm 0.01$–0.09 ± 0.01. However, the higher value of $\dot{m}_d$ compared to $\dot{m}_h$ and lower X_s, clearly indicates that the source moved to a soft spectral state. The shock compression ratio (R) varies between 5.5 ± 0.4 and 6.7 ± 0.6, and falls in the range where the theoretical mass outflow rate is much less (see S. K. Chakrabarti 1999). The mass of the BH (M_{BH}) was obtained from the fit ranges of 9.2 ± 1.0–$9.8 \pm 1.5\,M_\odot$ for both epochs, which are constant within the error bar and also agree with the kerrbb model-fitted BH mass. All model-fitted parameters are given in Table 3.

Given the JeTCAF model-fitted parameters, we have estimated the mass outflow rate for this source to be 0.011 ± 0.001 (minimum for the I+N1 parameters) and 0.022 ± 0.003 (maximum for N2 parameters) $\dot{M}_{Edd}$ using Equation (16) derived in S. K. Chakrabarti (1999). In our model, as discussed earlier, both the corona and the base of the jet behave as a Comptonizing medium. Such a low mass outflow rate also agrees with the soft spectral state.

The JeTCAF model-fitted hot accretion flow component ($\dot{m}_h$) that contributes to the power-law emission from the corona is approximately one-third of the cold thermal disk component ($\dot{m}_d$). Additionally, the size of the corona (X_s) is significantly small (6–9 r_S), compared to its size in the intermediate states which is $\gtrsim 60\,r_S$, phenomenologically estimated using timing (QPO) properties (K. Chatterjee et al. 2024). These estimates infer that the emission is dominated by the thermal disk rather than the corona. Therefore, the geometrical configuration and high disk mass accretion rate may explain that the observed low PD mainly comes from the accretion disk, where the polarization is perpendicular to the disk. Conversely, the PD contribution from the corona is expected to be less due to its smaller size loaded with higher mass, which can trap radiation by repeated scattering resulting in lower PD.

Subsequently, the unpolarized radiation from the central source scattered by the corona of radius X_s and height h_{shk} can gain a net fractional polarization, depending on i. Therefore, given the best-fitted corona geometry and i, one can estimate the PD using the relation (M. C. Begelman & C. F. McKee 1983) $\mathrm{PD} = \sin^2 i (1 - \mathcal{R}_c)/[2(1 + \mathcal{R}_c) + (1 - \mathcal{R}_c) \sin^2 i]$, where $\mathcal{R}_c = 2(h_{shk}/X_s)^2$. The h_{shk} is estimated using Equation (1) derived in D. Debnath et al. (2014). For the best-fitted model parameters in epoch I+N2, the above relation predicts an expected PD of $\sim$4%–6%. This range of PD was detected for other sources earlier (see Section 1) in their hard or intermediate spectral states, where the corona properties change and that can contribute more to polarization. Therefore, such predictions can be further verified in the future if the source can be observed in other spectral states independently by IXPE and India's recently launched X-ray Polarimeter Satellite (XPoSat) or jointly.

4. Conclusions

In this paper, we have performed spectropolarimetric studies of a recently discovered black hole X-ray binary Swift J151857 using simultaneous IXPE and NuSTAR observations on 2024 March 17 and 18. The key findings from this study are summarized below:

1. The first detection of X-ray polarization of the source using IXPE yields a PD and PA of $\sim 1.34\% \pm 0.27\%$ and $\sim -14^\circ.0 \pm 5^\circ.8$ in the soft spectral state. The PD value further supports that the changes in spectral states are possibly followed by changes in polarization properties.
2. The low PD measurement can be due to the low spin and inclination of the disk, which agrees with the previous detections. Additionally, in the SS, the corona has significantly shrunk increasing its optical depth and the emission is coming mainly from the disk. Therefore, it can significantly depolarize the emission by repeated scattering.
3. The low cutoff powerlaw energy ($\sim$36–78 keV) and high powerlaw photon index (>2.2) indicate a transition to a soft spectral state of the source. This is expected as the source ejected a high radio flare in the first week of March and later moved to the soft spectral state. The spectral state has further been confirmed from the nondetection of QPOs using Insight-HXMT observations during this epoch (K. Chatterjee et al. 2024).
4. Additionally, the high disk mass accretion rate compared to the hot flow rate with lower corona size ($\sim$6–9 r_S) supports the transition of the source to the soft spectral state.
5. The mass of the BH estimated from different model fits in a narrow range between 9.2 ± 1.0 and $10.1 \pm 1.7\,M_\odot$. The spin parameter of the source is $\sim 0.6 \pm 0.1$–0.7 ± 0.2 with an accretion disk inclination of $\sim 36^\circ \pm 7^\circ$–$46^\circ \pm 15^\circ$ for a source distance of 10 kpc.
6. We did not find a significant mass outflow rate ($<0.03\,\dot{M}_{Edd}$), which can be due to the transition of the source to the soft spectral state.

We have detected X-ray polarization of the source Swift J151857 for the first time in the soft spectral state and inferred the origin of polarization properties (PD and PA profiles). Our detailed study of the BHXRB source Swift J151857 sheds light on the accretion disk properties and the geometry of the corona, as well as the estimation of intrinsic properties of the BH. The estimated spin parameter and disk inclination can explain the low PD detection. Moreover, the joint IXPE and NuSTAR, and independent NuSTAR analysis show consistent results. A detailed timing study on this source further confirms the

spectral state of the source (K. Chatterjee et al. 2024). We have further predicted the PD using both model-fitted parameters, which is significantly high (4%–6%); however, in the range of the PD detected for other sources in their hard or intermediate states. Such predictions can be further verified in the future using IXPE and XPoSat, independently or jointly.

Acknowledgments

ORCID iDs

Santanu Mondal ● https://orcid.org/0000-0003-0793-6066
Kaushik Chatterjee ● https://orcid.org/0000-0002-6252-3750
Chandra B. Singh ● https://orcid.org/0000-0002-7782-5719

References

Arnaud, K. A. 1996, in ASP Conf. Ser. 101, XSPEC: The First Ten Years, ed. G. H. Jacoby & J. Barnes (San Francisco, CA: ASP), 17
Baglio, M. C., D'Avanzo, P., Ferro, M., et al. 2024, ATel, 16506, 1
Baldini, L., Bucciantini, N., Lalla, N. D., et al. 2022, SoftX, 19, 101194
Begelman, M. C., & McKee, C. F. 1983, ApJ, 271, 89
Belloni, T., Homan, J., Casella, P., et al. 2005, A&A, 440, 207
Brenneman, L. W., & Reynolds, C. S. 2006, ApJ, 652, 1028
Burridge, B. J., Miller-Jones, J. C. A., Bahramian, A., et al. 2024, ATel, 16538, 1
Carotenuto, F., & Russell, T. D. 2024, ATel, 16518, 1
Cavero, N. R., Marra, L., Krawczynski, H., et al. 2023, ApJL, 958, L8
Chakrabarti, S., & Titarchuk, L. G. 1995, ApJ, 455, 623
Chakrabarti, S. K. 1997, ApJ, 484, 313
Chakrabarti, S. K. 1999, A&A, 351, 185
Chakrabarti, S. K., Debnath, D., & Nagarkoti, S. 2019, AdSpR, 63, 3749
Chatterjee, K., Pujitha Suribhatla, S., Mondal, S., & Singh, C. B. 2024, arXiv:2406.17629
Chatterjee, R., Agrawal, V. K., Jayasurya, K. M., & Katoch, T. 2023, MNRAS, 521, L74
Chattopadhyay, I., & Das, S. 2007, NewA, 12, 454
Connors, P. A., Piran, T., & Stark, R. F. 1980, ApJ, 235, 224
Cowie, F. J., Carotenuto, F., Fender, R. P., et al. 2024, ATel, 16503, 1
Debnath, D., Chakrabarti, S. K., & Mondal, S. 2014, MNRAS, 440, L121
Debnath, D., Mondal, S., & Chakrabarti, S. K. 2015, MNRAS, 447, 1984
Del Santo, M., Russell, T. D., Marino, A., & Motta, S. 2024, ATel, 16519, 1
Done, C., Gierliński, M., & Kubota, A. 2007, A&ARv, 15, 1

Dovčiak, M., Muleri, F., Goosmann, R. W., Karas, V., & Matt, G. 2008, MNRAS, 391, 32
Fabian, A. C., Rees, M. J., Stella, L., & White, N. E. 1989, MNRAS, 238, 729
Haardt, F., & Maraschi, L. 1993, ApJ, 413, 507
Harrison, F. A., Craig, W. W., Christensen, F. E., et al. 2013, ApJ, 770, 103
Homan, J., Wijnands, R., van der Klis, M., et al. 2001, ApJS, 132, 377
Ingram, A., Ewing, M., Marinucci, A., et al. 2023, MNRAS, 525, 5437
Iwasawa, K., Fabian, A. C., Reynolds, C. S., et al. 1996, MNRAS, 282, 1038
Jana, A., & Chang, H.-K. 2024, MNRAS, 527, 10837
Jana, A., Debnath, D., Chakrabarti, S. K., Mondal, S., & Molla, A. A. 2016, ApJ, 819, 107
Joye, W. A., & Mandel, E. 2003, in ASP Conf. Ser. 295, Astronomical Data Analysis Software and Systems XII, ed. H. E. Payne, R. I. Jedrzejewski, & R. N. Hook (San Francisco, CA: ASP), 489
Kennea, J. A., Lien, A. Y., D'Elia, V., et al. 2024a, ATel, 16500, 1
Kennea, J. A., Lien, A. Y., & Page, K. L. 2024b, GCN, 35853, 1
King, A. R. 1998, MNRAS, 296, L45
Kislat, F., Clark, B., Beilicke, M., & Krawczynski, H. 2015, APh, 68, 45
Krawczynski, H. 2012, ApJ, 754, 133
Krawczynski, H., Muleri, F., Dovciak, M., et al. 2022, Sci, 378, 650
Kushwaha, A., Jayasurya, K. M., Agrawal, V. K., & Nandi, A. 2023a, MNRAS, 524, L15
Kushwaha, A., Jayasurya, K. M., & Nandi, A. 2023b, MNRAS: Lett., 524, L15
Li, L.-X., Narayan, R., & McClintock, J. E. 2009, ApJ, 691, 847
Li, L.-X., Zimmerman, E. R., Narayan, R., & McClintock, J. E. 2005, ApJS, 157, 335
Majumder, S., Kushwaha, A., Das, S., & Nandi, A. 2024, MNRAS, 527, L76
Marra, L., Brigitte, M., Rodriguez Cavero, N., et al. 2024, A&A, 684, A95
Mondal, S. 2020, AdSpR, 65, 693
Mondal, S., & Chakrabarti, S. K. 2013, MNRAS, 431, 2716
Mondal, S., & Chakrabarti, S. K. 2021, ApJ, 920, 41
Mondal, S., Chakrabarti, S. K., & Debnath, D. 2016, Ap&SS, 361, 309
Mondal, S., Chakrabarti, S. K., Nagarkoti, S., & Arévalo, P. 2017, ApJ, 850, 47
Mondal, S., Chatterjee, R., Agrawal, V. K., & Nandi, A. 2024, PASA, 41, e072
Mondal, S., Debnath, D., & Chakrabarti, S. K. 2014, ApJ, 786, 4
Mondal, S., & Jithesh, V. 2023, MNRAS, 522, 2065
Nandi, A., Debnath, D., Mandal, S., & Chakrabarti, S. K. 2012, A&A, 542, A56
Neilsen, J., & Homan, J. 2012, ApJ, 750, 27
Novikov, I. D., & Thorne, K. S. 1973, in Black Holes (Les Astres Occlus), ed. C. DeWitt & B. DeWitt (New York: Gordon and Breach), 343
Podgorny, J., Marra, L., Muleri, F., et al. 2023, MNRAS, 526, 5964
Podgorný, J., Svoboda, J., Dovčiak, M., et al. 2024, A&A, 686, L12
Ratheesh, A., Dovčiak, M., Krawczynski, H., et al. 2024, ApJ, 964, 77
Rawat, D., Garg, A., & Mendez, M. 2023, MNRAS, 525, 661
Remillard, R. A., & McClintock, J. E. 2006, ARA&A, 44, 49
Reynolds, C. S. 2019, NatAs, 3, 41
Saikia, P., Russell, D. M., Baglio, M. C., et al. 2024, ATel, 16516, 1
Schnittman, J. D., & Krolik, J. H. 2010, ApJ, 712, 908
Sguera, V. 2024, ATel, 16524, 1
Shui, Q. C., Yin, H. X., Zhang, S., et al. 2021, MNRAS, 508, 287
Sunyaev, R. A., & Titarchuk, L. G. 1980, A&A, 500, 167
Sunyaev, R. A., & Titarchuk, L. G. 1985, A&A, 143, 374
Svoboda, J., Dovčiak, M., Steiner, J. F., et al. 2024a, ApJL, 966, L35
Svoboda, J., Dovčiak, M., Steiner, J. F., et al. 2024b, ApJ, 960, 3
Taverna, R., Zhang, W., Dovciak, M., et al. 2020, MNRAS, 493, 4960
Tetarenko, B. E., Sivakoff, G. R., Heinke, C. O., & Gladstone, J. C. 2016, ApJS, 222, 15
Veledina, A., Muleri, F., Dovčiak, M., et al. 2023, ApJL, 958, L16
Veledina, A., Muleri, F., Poutanen, J., et al. 2024, NatAs, 8, 1031
Weisskopf, M. C., Ramsey, B., O'Dell, S., et al. 2016, Proc. SPIE, 9905, 990517
Wilms, J., Allen, A., & McCray, R. 2000, ApJ, 542, 914
Zhang, S.-N., Li, T., Lu, F., et al. 2020, SCPMA, 63, 249502